

# Green Speaker Design

## (Part 1: Optimal Use of System Resources)

Wolfgang Klippel KLIPPEL GmbH, Mendelssohnallee 30, 01277 Dresden, Germany

Increasing the efficiency and voltage sensitivity of the electro-acoustical conversion is the key to modern audio devices generating the required sound output with minimum size, weight, cost and energy. Traditional loudspeaker design sacrifices efficiency for sound quality. Nonlinear adaptive control can compensate for the undesired signal distortion, protect the transducer against overload, stabilize the voice coil position and cope with time-varying properties of the suspension. The paper presents a new design concept for active loudspeaker system that uses the new degree of freedom provided by DSP for exploiting a nonlinear motor topology, a soft suspension and modal vibration in the diaphragm, panel and in the acoustical systems.

### 1 Introduction

Customers of audio devices expect that the audio signal can be reproduced at sufficient amplitude and quality. However, compromises are made to satisfy additional preferences of smaller, lighter, and cheaper products with a longer battery life.

The progress of digital signal processing provides new opportunities for manipulating the input signal supplied to the loudspeaker to generate more sound output, a desired directivity, and less distortion while protecting the transducer actively against thermal and mechanical overload. Software can provide generic solutions with self-learning capabilities that monitor the properties of the transducer, generate the optimal control output and adaptively react to changing conditions. Furthermore, digital signal processing becomes, with higher integration, more affordable and can compete with paper, iron, neodymium and other loudspeaker materials.

This paper presents a new concept for designing special hardware components for active systems that exploit the new degrees of freedom provided by DSP. The optimal use of all resources such as material, energy, and manufacturing effort becomes more important than a passive system that generates a linear transfer behavior and low distortion in the output signal. This new concept, also called *Green Speaker Design*, uses the efficiency of the electro-acoustical conversion and voltage sensitivity as the key criteria for the speaker optimization. This causes a paradigm shift: Some nonlinearities inherent in the electro-dynamical loudspeaker are considered beneficial because they make the loudspeaker more efficient.

This new concept will be presented in two parts: The first part gives a short overview on the new software algorithms and develops the theoretical basis for the practical system design. The second part [1] is dedicated to the optimal transducer design. It investigates the influence of geometry, material properties, and other considerations. Finally, a practical case study applies the new concept to an existing transducer and shows the potential of the new technology.

### 2 Digital Signal Processing

This section summarizes the new opportunities provided by digital signal processing for loudspeakers:

Figure 1 shows adaptive, nonlinear control based on monitoring of the electrical input current  $i(t)$  that generates a desired transfer behavior between digital audio input  $w(t)$  and sound pressure output  $p(t)$  over the lifetime of the loudspeaker system.

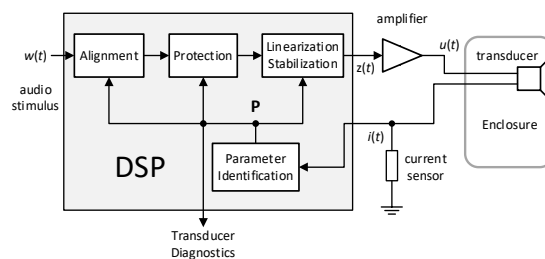


Figure 1: Active loudspeaker system with adaptive, nonlinear control of the transducer based on voltage and current monitoring

Linear filtering has been used for a long time to equalize amplitude response of the passive system to a desired target curve [2]. Active alignment of the passive loudspeaker system combines lumped parameter modeling with general filter design [3]. The original poles in the passive system can be canceled by zeros in the filter functions, and newly introduced poles virtually shift the cut-off frequency of the total system. This kind of active alignment of small closed box systems can generate a significant bass boost in the voltage signal.

Modern amplifiers can provide more power than the transducer can usually handle. To avoid mechanical and thermal overload, active protection systems [4], [5], [6] have been developed that detect a critical state and attenuate the input signal before damage occurs. In order to combine reliable protection with maximum output, an accurate prediction of voice coil displacement and voice coil temperature requires nonlinear and thermal modeling at high amplitudes [7].

The dominant nonlinearities inherent in electro-dynamical loudspeakers can be represented by

lumped parameters such as force factor  $Bl(x)$ , suspension stiffness  $K_{MS}(x)$ , mechanical resistance  $R_{MS}(v)$  and inductance  $L(x, i)$  depending on internal state variables voice coil displacement  $x$ , velocity  $v$  and input current  $i$ . This model generates a deterministic transducer behavior [8] and it is obvious to use this knowledge in nonlinear controllers to generate a pre-distorted audio signal  $z(t)$  containing compensation distortion, which cancels out the nonlinear distortion generated in the following loudspeaker attached. Thus, a linear transfer function  $H_o(f, r)$  describes the overall system not only in the small signal domain but also at high amplitudes.

The mirror filter [9] uses this property and synthesizes the voice coil displacement  $x(t)$  and other transducer state variables based on the electrical input signal  $w(t)$ . This nonlinear filter can compensate all of the transducer nonlinearities that are considered in the lumped parameter modeling. The feed-forward structure has a low complexity, is always stable and generates no latency in the audio signal.

Theoretically, the mirror filter needs no additional sensor for monitoring the transducer state. The free parameters in the mirror filter have a physical meaning and correspond to the linear and nonlinear transducer parameters. In practice, any mismatch between the control parameters in the mirror filter and actual transducer parameters will deteriorate the distortion cancelation [10]. Although the mirror filter can be operated with fixed parameters, an adaptive parameter identification [11] is required to cope with unavoidable production variances, aging of the suspension [12], changing climate conditions and other external influences [13].

All transducer parameters required for the mirror filter can be identified by an inexpensive sensor for monitoring the input current  $i(t)$  [14]. Thus, the mirror filter with current sensing becomes a self-learning control system that simplifies the tuning process in active systems and provides accurate transducer parameters over the lifetime of the product while reproducing music or other audio signals.

The adaptive nonlinear control can cope with undesired effects generated by a voice coil offset such as the generation of harmonic and intermodulation distortion, DC displacement and other instabilities [8]. If the power amplifier is DC coupled, the control system can actively stabilize the transducer [15] and keep the coil at the optimal position, giving maximum AC displacement and sound output.

Nowadays, the cost generated by hosting software algorithms ( $\approx 100$  MIPS) in silicon can compete with the benefits and cost savings generated on the transducer side, even in low-cost consumer applications.

### 3 Efficiency

However, digital signal processing cannot directly improve the efficiency of the electro-acoustical conversion, which is very poor in loudspeakers, headphones and other transducers. This characteristic plays a major role in Green Speaker Design where the influence of the audio signal  $w(t)$  is considered. This section provides the theoretical basis and useful expressions for the following discussion:

In general, the electro-acoustical efficiency is defined as the ratio

$$\eta = \frac{P_a}{P_e} 100\% \quad (1)$$

between electric input power  $P_e$  and the acoustic output power  $P_a$  for any stimulus such as a test signal or common audio signals.

The real input power  $P_e$  can be calculated in the time domain as the product of input current  $i(t)$  and open circuit amplifier output voltage (here called generator voltage  $u_g(t)$ ) averaged over a measurement interval:

$$P_e = \overline{u_g(t)i(t)} = \int_0^{+\infty} G_u^2(f) \Re(Z_E(f)^{-1}) df \quad (2)$$

This is equivalent to the squared voltage spectrum  $G_u^2(f)$  of an arbitrary stimulus multiplied by the real part of the electric input admittance  $Z_E(f)^{-1}$ .

The acoustic output power  $P_a$  can be determined by integrating the far-field sound pressure over a closed surface  $S$  around the transducer and expressing the result in the time and frequency domain as

$$\begin{aligned} P_a &= \frac{1}{\rho_0 c} \int_S \overline{p(t, \mathbf{r})^2} dS \\ &= \frac{1}{\rho_0 c} \int_0^{+\infty} G_u^2(f) |H(f, \mathbf{r}_{ref})|^2 Q(f, \mathbf{r}_{ref}) S df \end{aligned} \quad (3)$$

using the specific acoustic impedance  $\rho_0 c$ , the complex transfer function  $H(f, \mathbf{r}_{ref})$  between a sinusoidal generator voltage  $u_g$  and sound pressure  $p(t, \mathbf{r}_{ref})$  at the reference point  $\mathbf{r}_{ref}$  (usually at a distance  $r_{ref} = 1$  m on-axis from the source) and the directivity factor

$$Q(f, \mathbf{r}_{ref}) = \frac{S |p(f, \mathbf{r}_{ref})|^2}{\int_S |p(f, \mathbf{r})|^2 dS} \quad (4)$$

which describes the ratio between the power radiated by a virtual source generating the same sound pressure  $p(f, \mathbf{r}_{ref})$  at all points on a spherical surface  $S$  and the acoustical output power generated by the real source passing surface  $S$ .

The efficiency  $\eta$  in Eq. (1) can also be approximated by a mean value for a particular stimulus

$$\eta \approx \frac{\int_0^{+\infty} \eta(f) \Re(Z_E(f)^{-1}) G_u^2(f) df}{\int_0^{+\infty} \Re(Z_E(f)^{-1}) G_u^2(f) df} \quad (5)$$

using a frequency dependent efficiency factor

$$\eta(f) = \frac{|H(f, r_{ref})|^2 Q(f, r_{ref}) S}{\rho_0 c \Re(Z_E(f)^{-1})} 100\% \quad (6)$$

weighted by the voltage spectrum  $G_u(f)$  of the stimulus.

The frequency dependent efficiency factor  $\eta(f)$  corresponds to a previous discourse on loudspeaker efficiency based on linear modeling valid in the small signal domain [17].

#### 4 Voltage Sensitivity

A second important property of the transducer is the voltage sensitivity that can be defined in a general way as the total sound pressure level in dB

$$\begin{aligned} SPL_{u_{ref}, r_{ref}} &= 20 \lg \left( \frac{p_{rms}(r_{ref})}{p_0} \right) \\ &= 10 \lg \left( \frac{1}{p_0^2} \int_0^{+\infty} G_u^2(f) |H(f, r_{ref})|^2 df \right) \end{aligned} \quad (7)$$

at a given reference distance on-axis (typically  $r_{ref} = 1$  m) with the reference sound pressure  $p_0 = 2 \cdot 10^{-5}$  Pa generated by an arbitrary stimulus with known voltage amplitude spectrum  $G_u(f)$  corresponding to a reference rms-value of the generator voltage (typically  $u_{ref} = 1$  rmsV):

$$u_{ref}^2 = \int_0^{+\infty} G_u^2(f) df \quad (8)$$

The voltage sensitivity in Eq. (7) considers the properties of the stimulus and is a useful characteristic to calculate the peak voltage provided by the power amplifier.

For a sinusoidal stimulus at frequency  $f$ , a frequency dependent voltage sensitivity can be expressed as

$$SPL_{u_{ref}, r_{ref}}(f) = 20 \lg \left( |H(f, r_{ref})| \frac{u_{ref}}{p_0} \right) \quad (9)$$

which is a useful characteristic for transducer design and similar to the frequency response as defined in the IEC standard [21].

Comparing Eqs. (6) and (9) shows that efficiency and voltage sensitivity are related but are not identical. Both characteristics contain the on-axis transfer response  $H(f, r_{ref})$  that generates a similar curve shape at low and high frequencies. However, the electrical impedance  $Z_E(f)$  increases the efficiency at the resonance frequency  $f_s$ .

#### 5 Electro-mechanical Modeling

The further investigations are performed on an electro-dynamic transducer using a moving coil in a static magnetic field. A lumped parameter model [3] as shown in Figure 2 can be used to describe the transducer at low frequencies while neglecting effects of lossy inductance, visco-elastic creep, modal vibrations and wave propagation that require a more complex model.

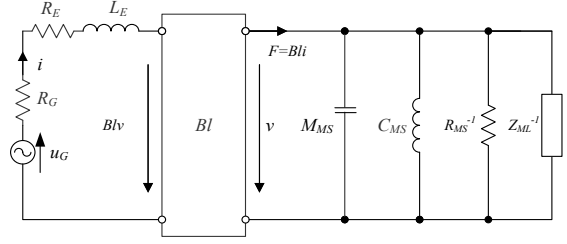


Figure 2: Lumped parameter model with impedance-mobility analogy of an electro-dynamical transducer with amplifier output

##### 5.1 Small Signal Modeling

The electro-acoustic transfer function  $H(j\omega, r)$  between the sinusoidal generator voltage  $u_g$  and the sound pressure  $p(r)$  generated on-axis at a distance  $r$  can be modeled at small displacement  $x \approx 0$  as:

$$\begin{aligned} H(j\omega, r) &= \frac{p(r)}{u_g} \\ &= H_v(j\omega) H_a(j\omega) H_{rad}(j\omega, r) \end{aligned} \quad (10)$$

The first transfer function describes the relationship between generator voltage  $u_g$  and coil velocity  $v$  as

$$\begin{aligned} H_v(j\omega) &= \frac{v}{u_g} \\ &= \frac{Bl}{(R_E + R_g + j\omega L_E) Z_{MT} + (Bl)^2} \end{aligned} \quad (11)$$

using the force factor  $Bl$ , DC resistance  $R_E$ , generator resistance  $R_g$ , voice coil inductance  $L_E$  and the total mechanical impedance:

$$Z_{MT} = \frac{F}{v} = R_{MS} + j\omega M_{MS} + \frac{K_{MS}}{j\omega} + Z_{ML} \quad (12)$$

The impedance  $Z_{MT}$  considers the mechanical resistance  $R_{MS}$ , the total moving mass  $M_{MS}$  and suspension stiffness  $K_{MS}$  including air load and an additional impedance  $Z_{ML}$  representing an equivalent load generated by other mechanical or acoustical components (e.g. passive radiator, box).

The second transfer function

$$H_a(j\omega) = \frac{q_a}{v} \quad (13)$$

describes the relationship between velocity  $v$  and volume velocity  $q_a$  generating the acoustical output power:

$$P_a(\omega) = \left| \frac{q_a}{\sqrt{2}} \right|^2 R_{AR}(\omega) \quad (14)$$

The real part of the acoustical radiation impedance can be approximated by

$$R_{AR}(\omega) = \frac{\rho_0 c}{S_D} \left( 1 - \frac{J_1(2ka)}{ka} \right) \approx \begin{cases} \frac{\omega^2 \rho_0}{2\pi c} & |ka| < 0.5 \\ \frac{\rho_0 c}{S_D} & |ka| > 5 \end{cases} \quad (15)$$

using the density of air  $\rho_0$ , the Bessel function of the first kind  $J_1$ , the wavenumber  $k=\omega/c$  and the radius  $a$  of the round effective radiator's surface  $S_D$  [16].

The third transfer function  $H_{rad}(\omega, r)$  describes the radiation of a monopole injecting volume velocity  $q_a$  into the half-space and generating the on-axis sound pressure  $p(r)$  at distance  $r$  as:

$$H_{rad}(j\omega, r) = \frac{p(r)}{q_a} = \frac{j\omega \rho_0}{2\pi r} e^{-jkr} \quad (16)$$

Eq. (16) is a valid approximation under the condition that the wavelength is larger than the circumference of the radiating surface and the source is close to a wall and other large boundary. At higher frequencies, multiple monopoles (Rayleigh equation) and additional dipoles (Kirchhoff-Helmholtz equation) have to be placed on the radiating surface to calculate the sound radiation with sufficient accuracy (Boundary Element Method [18]).

The efficiency can be described by

$$\eta(f) = \frac{|H_v(j\omega)H_a(j\omega)|^2 R_{AR}(j\omega)}{\Re(Z_E(j\omega)^{-1})} 100\% \quad (17)$$

with the electrical input impedance:

$$Z_E = R_E + R_g + j\omega L_E + (Bl)^2 \left( Z_{MT}(j\omega) - \frac{(Bl)^2}{R_E + R_g} \right)^{-1} \quad (18)$$

Here in this paper it is assumed that the output impedance of the amplifier  $R_g$  is much smaller than the DC resistance  $R_E$ .

## 5.2 Large Signal Modeling

At higher amplitudes, the force factor product  $Bl$ , suspension stiffness  $K_{MS}$  and voice coil inductance  $L_E$  are not constant values but become nonlinear functions  $Bl(x)$ ,  $K_{MS}(x)$  and  $L_E(x)$  depending on instantaneous voice coil displacement  $x$ . For a particular stimulus generating a voice coil displacement  $x$  with the probability density function  $pdf(x)$ , an effective force factor

$$\overline{Bl} = \int_{-\infty}^{\infty} Bl(x) pdf(x) dx \quad (19)$$

an effective stiffness of the suspension

$$\overline{K_{MS}} = \int_{-\infty}^{\infty} K_{MS}(x) pdf(x) dx \quad (20)$$

and an effective voice coil inductance

$$\overline{L_E} = \int_{-\infty}^{\infty} L_E(x) pdf(x) dx \quad (21)$$

can be introduced.

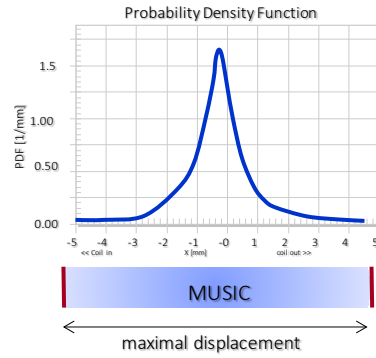


Figure 3: Probability Density Function  $pdf(x)$  of voice coil displacement  $x$  for a typical audio signal (e.g. music)

Figure 3 shows an example of the  $pdf(x)$  of typical audio material representing most music genres and speech. This bell-shaped characteristic shows that the coil is close to the rest position most of the time, and high peak values are relatively rare. Thus, from a statistical perspective, the effective parameters  $\overline{Bl} \approx Bl$ ,  $\overline{K_{MS}} \approx K_{MS}$ ,  $\overline{L_E} \approx L_E$  are close to the nonlinear parameter values found at the rest position  $x=0$ , and the small signal efficiency and voltage sensitivity are also useful approximations for higher amplitudes.

## 6 Mechano-Acoustical System

This paper considers passive loudspeaker systems that are comprised of one transducer and other hardware components such as a baffle, cabinet, panel or an additional mechanical resonator to generate the required sound power output at maximum efficiency while providing sufficient sensitivity to cope with the limited peak voltage capabilities of the amplifier.

### 6.1 Closed-box System

Mounting the transducer in an almost sealed cabinet leads to a compact loudspeaker system where the acoustical cancellation between the air flow radiated from the rear and front side of the diaphragm is avoided.

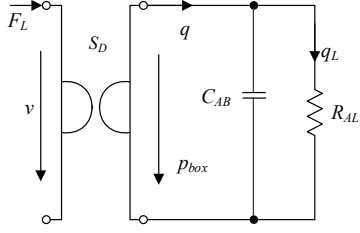


Figure 4: Lumped parameter model of the closed-box system based on mobility and acoustical impedance analogy

The mechanical load  $Z_{ML}$  generated by a closed box is highly reactive and can be described at small amplitudes as

$$Z_{ML} = \frac{S_D^2 R_{AL}}{1 + j\omega R_{AL} C_{AB}} \quad (22)$$

based on the lumped parameter model shown in Figure 4. The acoustical compliance can be expressed as

$$C_{AB} = \frac{V_{AB}}{\kappa p_0} \quad (23)$$

with the air volume  $V_{AB}$  in the box, the static air pressure  $p_0$  and the adiabatic coefficient  $\kappa = 1.4$ . The resistance  $R_{AL}$  represents the internal lining, a leak or an intended barometric vent that ensures an exchange with ambient static air pressure.

Neglecting the acoustic resistance  $R_{AL}$  the impedance becomes

$$Z_{ML}(j\omega) \approx \frac{S_D^2}{j\omega C_{AB}} = \frac{S_D^2 \kappa p_0}{j\omega V_{AB}} \quad (24)$$

and the source transfer function

$$H_a(\omega) = \frac{q_a}{v} = \frac{q_c}{v} \approx S_D \quad (25)$$

can be approximated by the effective radiation area  $S_D$ .

The voltage sensitivity  $SPL(f)$  rises with 12dB/oct. with frequencies below the fundamental system resonance  $f_0$  defined as:

$$f_0 = \frac{1}{2\pi} \sqrt{\frac{1}{M_{MS}} \left( \frac{S_D^2}{C_{AB}} + K_{MS} \right)} \quad (26)$$

The system resonance  $f_0$  is only slightly higher than the transducer resonance  $f_s$  in free air when the air volume  $V_{AB}$  is significantly higher than the equivalent air volume  $V_{AS}$  representing the mechanical stiffness  $K_{MS}$  in Eq. (12). Those large closed box systems can be realized by using available space such as the door cavity in automotive applications. A transducer with a softer suspension would be beneficial for a subwoofer operated in the frequency band  $f_0/3 < f < 2f_0$ .

However, a small volume  $V_{AB}$  is desirable in most applications and generates a high fundamental system resonance  $f_0$ , giving a poor bass performance. The

undesired low-frequency performance can be compensated by an electrical equalization in the controller generating a bass boost in the generator voltage  $u_g$ . In practice, the cut-off frequency  $f_c$  of the total system function  $H_o(j\omega, r)$  between controller input  $w(t)$  and sound pressure output  $p(t)$  can be shifted by 1-2 octaves downwards by using an efficient transducer and matching the voltage sensitivity to the amplifier capabilities.

If the stiffness  $K_{MB}$  generated by the small air volume  $V_{AB}$  is much larger than the mechanical stiffness  $K_{MS}$ , the efficiency at low frequencies  $f < f_0$  can be calculated as:

$$\eta(f) \approx (2\pi f)^4 \frac{\rho_0 (Bl)^2 V_{AB}^2}{2\pi c R_E (p_0 \kappa)^2 S_D^2} \quad (27)$$

It is interesting to note that a smaller radiation area  $S_D$  would increase the efficiency below system resonance frequency  $f_0$ , but would require a larger voice coil displacement  $x$  to generate the same volume velocity  $q_a$  at those frequencies. This design consideration would be only beneficial for closed-box subwoofers which are operated at low frequencies.

For wide-band loudspeaker, a maximum value of the  $S_D$  improves the passband efficiency and can be traded for the poor efficiency at low frequencies. Placing porous absorbing material (e.g. charcoal) inside the box reduces the resistance  $R_{AL}$ , and the volume velocity  $q_L$  bypasses the acoustical compliance  $C_{AB}$  and virtually increases the volume of the box.

The closed-box system shows also some undesired behavior at high amplitudes:

The AC sound pressure  $p_{box}$  inside small enclosures can exceed 140 dB and generate a nonlinear dependency of the compliance  $C_{AB}(p_{box})$  versus the sound pressure  $p_{box}$  which generates nonlinear harmonic distortion and a DC pressure that moves the coil outwards where the acoustical compliance is higher. This DC pressure will push air particles outwards through the leak represented by  $R_{AL}$  until the nonlinear force is compensated. If the high AC pressure is reduced, the coil moves inwards and air particles will flow into the box again. Thus, a variation of high AC pressure in a leaky box generates a transient DC component in pressure and voice coil displacement. Asymmetrical nonlinearities in the transducer will also generate a DC excitation force that only sees the mechanical stiffness  $K_{MS}$  because the leaky box is effectively open at low frequencies.

These undesired effects can be compensated by nonlinear control [15] using information provided by monitoring the input current.

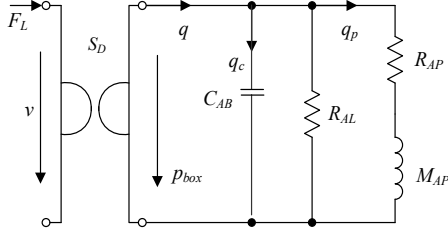


Figure 5: Lumped parameter model of a vented-box system based on mobility and acoustical impedance analogy.

## 6.2 Vented-Box System

A vented-box system modeled by an equivalent circuit in Figure 5 generates a significant acoustical load in the mechanical domain

$$Z_{ML}(j\omega) = Z_{ML,vent}(j\omega) = \frac{S_D^2}{j\omega C_{AB} + 1/R_{AL} + 1/(j\omega M_{AP} + R_{AP})} \quad (28)$$

at the port resonance frequency

$$f_p = \frac{1}{2\pi\sqrt{C_{AB}M_{AP}}} \quad (29)$$

where the reactive components generated by port mass  $M_{AP}$  and air compliance  $C_{AB}$  cancel each other. The force  $F_L$  provided by the transducer compensates for the losses generated by the leakage resistance  $R_{AL}$  and port resistance  $R_{AP}$ . The geometry of the enclosure and the port determines the port resonance frequency  $f_p$ .

The source transfer function

$$H_a(j\omega) = \frac{q_a}{v} = \frac{q_c}{v} = Z_{ML,vent} \frac{j\omega C_{AB}}{S_D} \quad (30)$$

between voice coil velocity  $v$  and volume velocity  $q_c$  has a high-pass characteristic, which reduces the efficiency and voltage sensitivity at frequencies below  $f_p$  and limits the usable frequency band at lower frequencies. Contrary to the closed-box system, an active equalization and a virtual shift of the cut-off frequency is less practical due to the steep slope of 24 dB/octave below the port resonance  $f_p$ .

The port resistance  $R_{AP}(q_p)$  rises by a nonlinear function with the volume velocity  $q_p$  in the port and reduces the quality factor  $Q_p$  at higher amplitudes significantly. The cross-sectional area  $S_p$  of the port should be large enough to keep the nonlinear effects and the air turbulences acceptable.

Different shapes of inner and outer orifices and a close distance of the inner outlet to the cabinet walls can generate an asymmetrical port resistance  $R_{AP}(q_p)$  that rectifies the AC volume velocity  $q_p$  and generates dynamically a DC component in the pressure  $p_{box}$  and in the voice coil displacement  $x$ . The active stabilization of the voice coil can detect an offset and actively compensate for this effect and for the DC

displacement generated by other asymmetrical transducer nonlinearities [8].

Compared to a closed-box system, the vent reduces the voice coil velocity  $v$  and generates a smaller back EMF on the electrical side which improves the voltage sensitivity  $SPL(f)$  at frequencies close to  $f_p$ . The resonance also reduces the voice displacement  $x$ , which activates the transducer nonlinearities  $Bl(x)$ ,  $K_{MS}(x)$  and  $L_E(x)$  less. Thus, the distortion cancellation provided by the nonlinear control system is less active in vented enclosures compared to sealed enclosures.

## 6.3 Band-Pass System

The band-pass system uses a vented box on one side of the transducer and a sealed box on the other side. The mechanical load seen by the transducer can be described based on the lumped parameter model in Figure 6 as an impedance

$$Z_{ML} = \frac{S_D^2}{j\omega C_{AF} + 1/(j\omega M_{AP} + R_{AP})} + \frac{S_D^2}{j\omega C_{AB}} \quad (31)$$

using the acoustical compliance  $C_{AF}$  of the ported front volume  $V_{AF}$ , the mass  $M_{AP}$  and the resistance  $R_{AP}$  representing the port as discussed in section 6.2 and the acoustical compliance  $C_{AB}$  of the air in the rear volume  $V_{AB}$  behind the diaphragm while neglecting the losses in the box represented by resistance  $R_{AL}$ .

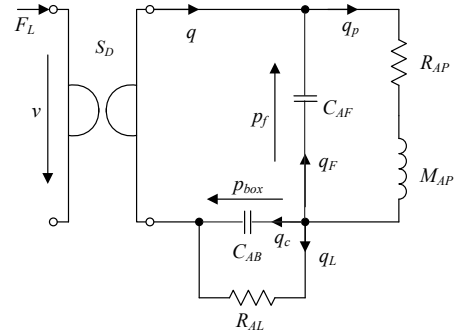


Figure 6: Acoustical equivalent circuit of a band-pass system using a rear and ported front volume.

The source transfer function

$$H_a(j\omega) = \frac{q_a}{v} = \frac{q_p}{v} = \frac{S_D}{j\omega C_{AF} (j\omega M_{AP} + R_{AP}) + 1} \quad (32)$$

between the coil velocity  $v$  and port volume velocity  $q_p$  has a low-pass characteristic falling with 12 dB/octave above the port resonance frequency:

$$f_p = \frac{1}{2\pi\sqrt{C_{AF}M_{AP}}} \quad (33)$$

The fundamental system resonance frequency  $f_0$  in the total transfer function  $H(\omega, r)$  in Eq. (10) can be calculated by equation:

$$f_0 = \frac{1}{2\pi} \left( \left( C_{AB} + \frac{S_D^2}{K_{MS}} \right) \left( M_{AP} + \frac{M_{MS}}{S_D^2} \right) \right)^{-1/2} \quad (34)$$

The design considerations for the transducer and for the rear volume  $V_{AB}$  discussed for the closed-box system in section 6.1 also apply for the band-pass system below  $f_0$ .

The resonance frequencies  $f_0$  and  $f_p$  determine the passband in the overall transfer function  $H(\omega)$ , which falls to lower and higher frequencies outside this band by 12 dB/octave. In woofer applications, where the bandwidth  $f_p - f_0$  is relatively small, the port resistance  $R_{AP}$  has a high influence on the sensitivity and efficiency in the passband. Modern micro-speaker with a rear volume and a side-fire port in the front volume are also bandpass systems wherein the port resonance is located at higher frequencies than the fundamental resonance (typically  $f_p > 4f_0$ ). In this case, the port mass  $M_{AP}$  is a critical system parameter, reducing the efficiency and voltage sensitivity in the passband.

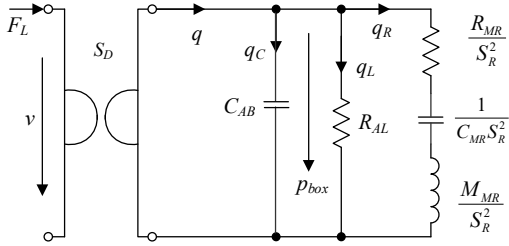


Figure 7: Acoustical equivalent circuit of a passive radiator system

#### 6.4 Passive Radiator System

The passive radiator system is an interesting alternative to the vented-box system because a lower cut-off frequency can be realized, giving a better bass performance in smaller cabinets. The vent is replaced by a mechanical resonator represented by the mass  $M_{MR}$ , compliance  $C_{MR}$  and resistance  $R_{MR}$  in the acoustical equivalent circuit shown in Figure 7. The mechanical load seen by the transducer becomes

$$Z_{ML}(j\omega) = Z_{ML,pr}(j\omega) = S_D^2 \left( \frac{j\omega C_{AB} + 1/R_{AL}}{+S_R^2 / (1/(j\omega C_{MR}) + j\omega M_{MR} + R_{MR})} \right)^{-1} \quad (35)$$

and the source transfer function is:

$$H_a(j\omega) = \frac{q_a}{v} = \frac{q_C}{v} = Z_{ML,pr} \frac{j\omega C_{AB}}{S_D} \quad (36)$$

The box compliances  $C_{AB}$  and the moving mass  $M_{MR}$  of the radiator generate a resonance frequency

$$f_p = \frac{S_R}{2\pi\sqrt{C_{AB}M_{MR}}} \quad (37)$$

that effectively limits the usable frequency band at lower frequencies. It is a clear benefit of the passive radiator system compared to the vented-box design

that the resonance frequency  $f_p$  can easily be tuned to low frequencies by using a heavier cone without increasing the size of the system. The passive radiator generates much less air noise than a vent of similar size.

The mechanical suspension of the passive radiator has a nonlinear compliance  $C_{MR}(x_R)$  which limits the excursion  $x_R$  at high amplitudes. If the artistic design and other practical restrictions do not allow a passive protection, the electric control system can also provide an active solution by predicting the excursion  $x_R$  and attenuating the input signal before an overload situation occurs.

#### 6.5 Panel System

The vented-box and passive radiator systems are good examples of how additional mechanical or acoustical resonators can improve the efficiency and voltage sensitivity of the loudspeaker system by increasing the real part of the load impedance  $Z_{ML}$  and canceling undesired reactive components (e.g. box compliance  $C_{AB}$ ). Additional poles in the transfer function in Eq. (10) can be also generated by a transmission line, flat panel or an additional high-frequency cone glued to the normal cone in the full-band transducer. The diaphragm or a thin cone also exhibits modal vibration at higher frequencies after breakup.

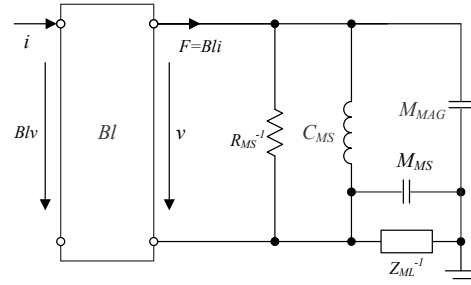


Figure 8: Lumped parameter model of a flat panel system based on impedance and mobility analogy

The cultivation of those resonances will be discussed on the particular example of a flat-panel system which here comprises only one exciter mounted on a panel that is glued in a rigid frame such as a modern display in a smart-phone. Those systems can be represented by the equivalent circuit [19] shown in Figure 8.

It is assumed that the total mass  $M_{MAG}$  of magnet, iron path and frame of the exciter is much higher than the moving mass of the exciter or the frame of the exciter is rigidly clamped with respect to the panel [20]. Then, the additional mechanical load  $Z_{ML}$  seen by the exciter corresponds to the mechanical impedance  $Z_{MP,FP}(r_c)$  of the panel at point  $r_c$ :

$$Z_{ML}(j\omega) = Z_{ML,FP}(j\omega, \mathbf{r}_e) = \left( \sum_{n=0}^N \frac{j\omega \Psi_n^2(\mathbf{r}_e)}{M_n (\omega_n^2 - \omega^2 + j2\zeta_n \omega \omega_n)} \right)^{-1} \quad (38)$$

Eq. (38) expands the total vibration into a superposition of  $N$  orthogonal modes where each mode of order  $n$  is characterized by the displacement given by the normalized mode shape  $\Psi_n(\mathbf{r}_e)$  at the excitation point  $\mathbf{r}_e$ , a natural frequency  $\omega_n$ , a modal damping ratio  $\zeta_n$  and a modal mass  $M_n$ .

The moving mass  $M_{MS}$  of the exciter limits the efficiency and voltage sensitivity at higher frequencies if:

$$|j\omega M_{MS}| > |Z_{ML}(j\omega)| \quad (39)$$

The transfer function  $H_a(f)$  between voice coil velocity  $v$  and equivalent source of volume velocity  $q_a$  modeled as

$$H_a(j\omega) = \frac{q_a}{v} = S_D(j\omega) = \sum_{n=0}^N \frac{Z_{ML,FP} j\omega \Psi_n(\mathbf{r}_e)}{M_n (\omega_n^2 - \omega^2 + j2\zeta_n \omega \omega_n)} \int_S \Psi_n(\mathbf{r}) dS \quad (40)$$

can be interpreted as an effective radiation area  $S_D(j\omega)$ , which is frequency dependent and can exceed the size  $S$  of the panel at higher frequencies:  $|S_D(j\omega)| > S$ .

The poles in Eq. (40) improve the efficiency and voltage sensitivity but generate undesired peaks in the frequency response. A linear IIR filter generating zeros in the overall response at frequencies  $\omega_n$  with quality factors  $Q_n=1/2\zeta_n$  can be used to equalize the overall transfer function  $H_o(f)$ .

The integral of the mode shape  $\Psi_n(\mathbf{r})$  over the radiation surface  $S$  can generate undesired zeros in  $H_a(f)$  if regions of positive and negative displacement of  $\Psi_n(\mathbf{r})$  provide equal contributions to the volume velocity  $q_a$ .

The excitation point  $\mathbf{r}_e$  should be not placed at nodal lines in the mode shapes  $\Psi_n(\mathbf{r}_e)$  in order to maximize the transfer function  $H_a(j\omega)$  over a wide frequency range.

The density of the panel material should be as low as possible to minimize the modal mass  $M_n$  and maximize  $H_a(f)$ . The thickness of the panel should be relatively thin to generate low bending stiffness that reduces the lowest natural frequency  $\omega_0$  and increases the density of the modes at higher frequencies.

Finite element analysis can be used to find the optimal geometry and material generating the desired modal properties.

## 7 Practical System Design

This section describes the procedure of the *Green Speaker Design* from the perspective of the system

integration as illustrated in Figure 9. It is the target to specify all components and to ensure the optimal use of the resources. A set of physical characteristics will be defined for transducer design as discussed in Part 2 [1].

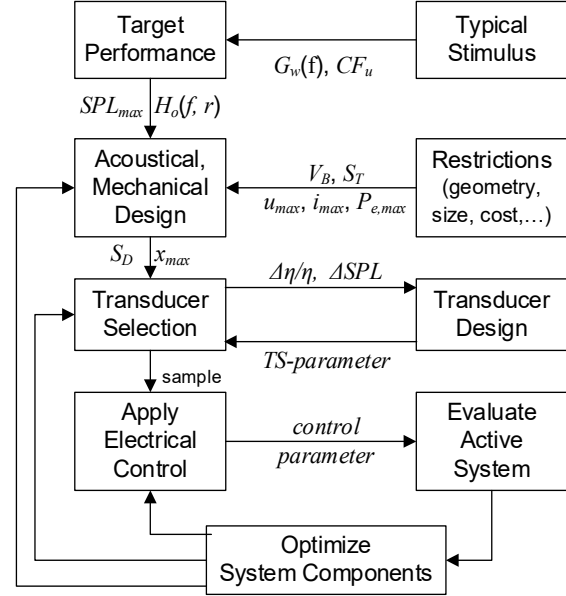


Figure 9: Overview of the practical design process

### 7.1 Target Performance Specification

The design process starts with the specification of two important characteristics

- maximum sound pressure level  $SPL_{max}(r)$  and
- desired frequency response  $H_o(f, r)$  of the overall system.

The active loudspeaker system shall be capable generating a maximum sound pressure level  $SPL_{max}(r)$ , in accordance with IEC 60268-21 [21], at a distance  $r$  on-axis while using a broadband audio stimulus (music, speech) that is typical for the particular application. The stimulus may be bandlimited to consider the crossover in a multi-way system. This stimulus is characterized by a long-term amplitude spectrum  $G_w(f)$  and a crest factor  $CF_w$ .

The nonlinear control reduces the harmonics, intermodulation and other nonlinear distortion and generates a desired linear relationship between digital audio input  $w(t)$  and sound pressure output  $p(t)$  at distance  $r$  as shown in Figure 1.

The overall transfer function  $H_o(f, r)$  can be specified by desired characteristics such as cut-off frequency  $f_c$ , quality factor, alignment type (e.g. Butterworth) or as a frequency response. The overall transfer function  $H_o(f, r)$  is time invariant as long as

an active protection of the transducer against mechanical and thermal overload is not required.

The spectrum  $G_w(f)$  of the typical program material is scaled at the control input to generate maximum sound pressure level output:

$$SPL_{\max} = 20 \lg \left( \frac{1}{p_0} \int_0^{+\infty} G_w(f) |H_o(f)| df \right) \quad (41)$$

The design process has to consider additional restrictions and particular requirements in the target application such as

- available box size (volume  $V_B$ ),
- total radiation area  $S_T$  including diaphragm area  $S_D$ , passive radiator area  $S_R$ , and panel size,
- maximum peak voltage  $u_{\max}$ ,
- maximum peak current  $i_{\max}$ ,
- maximum electrical power  $P_{e,\max}$  and
- other constraints (price, weight, ...).

The maximum peak voltage  $u_{\max}$  is usually limited by the rail voltage and the peak current  $i_{\max}$  by the FETs in the H-bridge of the class-D power amplifier. The maximum electrical power  $P_{e,\max}$  can be supplied from the amplifier to the transducer continuously (100h) without causing a thermal overload either in the amplifier output stage, power supply or in the voice coil [21].

Table 1: Overview of the pros (+) and cons (-) in the passive loudspeaker system used with nonlinear control

Passive Loudspeaker System	Small Size	Small Radiator	Equalization $f < f_0$	Sensitivity	Efficiency	Low Cost
Closed-Box	+	+	+	-	-	+
Vented-Box	-	+	-	+	+	+
Passive Radiator	+	-	-	+	+	-
Band-Pass	-	+	+	+	+	+
Panel	-	-	+	+	+	+

## 7.2 Passive System Design

The second step in the design procedure is the selection of the system type. Table 1 shows a selection of the most popular passive system types discussed in section 6 and their pros and cons for a final application:

The closed-box and the band-pass system are the best candidates for active equalization to shift the cut-off frequency  $f_c$  from the fundamental system

resonance  $f_0$  down by 1-2 octaves while using a small box volume and radiation area  $S_T$ . This kind of virtual bass extension cannot be realized in vented-box and passive radiator systems due to the steeper roll-off. However, the additional resonator is preferred in portable and professional applications where efficiency and voltage sensitivity are critical. The panel system represents any other distributed mode system using available components (e.g. display) as a radiator.

After selecting the optimal system type, the size and shape of the acoustical and mechanical elements (port, front volume, rear volume, panel) are designed for the given box size and total radiation area  $S_T$ . The peak value of air particle velocity  $v_{pk}$  in the port should be below a critical value (usually 10 m/s). This can be calculated, for example, in a bandpass system as

$$v_{pk} = v_{rms} 10^{CF_x/20} \quad (42)$$

with rms value

$$v_{rms}^2 = \int_0^{+\infty} \left| \frac{G_w(f) H_o(f)}{S_p H_{rad}(f)} \right|^2 df \quad (43)$$

depending on the stimulus spectrum  $G_w(f)$ , the radiation transfer function  $H_{rad}(f)$  in Eq. (16), the desired overall transfer function  $H_o(f)$  and the crest factor  $CF_x \approx CF_w$ .

In a similar way, the optimal parameters of the passive radiator or the flat panel shall be designed according to the considerations presented in section 6.

After the poles and zeros in the load impedance  $Z_L(f)$  and mechano-acoustical transfer function  $H_a(f)$  are determined, the optimal radiation area  $S_D$  of the transducer can be found by searching for a permissible peak value of the voice displacement  $x_{pk}$  that generates the desired output value  $SPL_{\max}$ . The relationship between  $S_D$  and  $x_{pk}$  depends on the acoustical system, the alignment and the stimulus. However, for a given  $S_D$  the transfer function  $H_a(f)$  is clearly defined and the peak displacement can be calculated as

$$x_{pk} = x_{rms} 10^{CF_x/20} \quad (44)$$

with the crest factor  $CF_x \approx CF_w$  and the rms-value of the displacement:

$$x_{rms}^2 = \int_0^{+\infty} \left| \frac{G_w(f) H_o(f)}{2\pi f H_{rad}(f) H_a(f)} \right|^2 df \quad (45)$$

## 7.3 Optimal Transducer Selection

In the third step of the design, a first candidate is selected from available transducers that meets the specified values for diaphragm area  $S_D$ , peak excursion  $x_{pk} < x_{mech}$  and other restrictions (size,

shape, price, weight). According to IEC standard 62458 [22], the maximal displacement  $x_{mech}$  describes the positive and negative limits of the useable working range where no mechanical limiting, voice coil rubbing or other impulsive distortion are generated.

If there are none available that fulfill those geometrical requirements, then a different type of the mechano-acoustical system should be considered or the target performance should be corrected.

The performance of the transducer in the active system can be predicted by using the linear, nonlinear and thermal parameters of an existing sample or a virtual design choice.

For most applications, the optimal transducer should have maximum efficiency, high voltage sensitivity and a symmetrical decay of the force factor nonlinearity  $Bl(x)$  down to 50 % of the maximum value  $Bl(x=0)$  at the peak excursion  $x_{pk}$ . If this motor is combined with a relatively soft suspension then the crest factor of control output signal will only marginally increase (typically  $CF_u \approx CF_w + 2$  dB) by the distortion cancellation signal added in the mirror filter to the stimulus  $w(t)$ .

Using the TS-parameters, the transfer function  $H(f)$  in Eq. (10) can be calculated, and the performance of the transducer under nonlinear control with the typical stimulus can be estimated.

If the electrical input power of the transducer calculated based on Eq. (2) as

$$P_e = \int_0^{+\infty} G_w^2(f) \Re(Z_E(f)^{-1}) \left| \frac{H_o(f)}{H(f)} \right|^2 df < P_{e,max} \quad (46)$$

exceeds the permissible limit value  $P_{e,max}$ , a more efficient transducer has to be selected or designed.

The transducer efficiency should also be improved if the peak values of both terminal voltage and input current

$$\begin{aligned} u_{pk} &= u_{rms} 10^{CF_u/20} < u_{max} \\ i_{pk} &= i_{rms} 10^{CF_i/20} < i_{max} \end{aligned} \quad (47)$$

with rms values

$$u_{rms}^2 = \int_0^{+\infty} G_w^2(f) \left| \frac{H_o(f)}{H(f)} \right|^2 df \quad (48)$$

$$i_{rms}^2 = \int_0^{+\infty} \left| \frac{G_w(f)}{Z_E(f)} \frac{H_o(f)}{H(f)} \right|^2 df \quad (49)$$

exceed the permissible limits  $u_{max}$  and  $i_{max}$ , respectively. Eq. (47) can use the crest factor  $CF_i \approx CF_u$  of the voltage signal for the current signal. If only the voltage capability of the amplifier is not sufficient, the voltage sensitivity can be improved by reducing the DC resistance  $R_E$ . Similarly, a higher  $R_E$  value can reduce the peak current  $i_{pk}$ .

Thus, the real input power  $P_e$  and the peak voltage and peak current in Eqs. (46) and (47) are the key criteria for selecting the optimal transducer for a particular application. The communication between transducer manufacturer and system integrator can be based on the required improvement of the efficiency

$$\frac{\Delta\eta}{\eta} = \left( \frac{P_e}{P_{e,max}} - 1 \right) 100\% \quad P_e > P_{e,max} \quad (50)$$

and the required improvement in the voltage sensitivity in dB:

$$\Delta SPL = 20 \lg \left( \frac{u_{pk}}{u_{max}} \right) \quad u_{pk} > u_{max} \quad (51)$$

The details of the transducer optimization are discussed in Part 2 [1]. It is interesting to note that the design choices can be investigated by finite element analysis and evaluated on the basis of lumped transducer parameters as defined in this paper. No real prototype has to be built and measured up to this point.

If the transducer manufacturer cannot further increase the efficiency of the transducer intended for the particular application, the system integrator has to check the previous steps in the design procedure and should consider changes in the target specification, alternative transduction principles or alternative system types.

## 7.4 Electrical Control

In the fourth step of the Green Speaker Design, a real sample of the transducer is required and mounted in the passive system.

If the nonlinear control is activated at the passive loudspeaker system for the first time, a non-recurring identification process (similar to the Large Signal Identification [23]) is automatically activated. This measures the linear, nonlinear and thermal parameters of the transducer mounted in the passive system and determines the permissible working range based on generic protection values such as nonlinear parameter variation ( $Bl_{min}$ ,  $C_{min}$ ), maximal increase of voice coil temperature  $T_{max}$  and maximal electrical input power  $P_{e,max}$ .

## 7.5 Active System Evaluation

The identified transducer parameters are stored and used as initial control parameters after powering up the controlled loudspeaker system of any unit of the same type. The adaptive control with current monitoring provides updated parameters and diagnostic information about the internal state of the particular device while reproducing natural audio stimuli and artificial test signals.

The target performance is evaluated by monitoring the input power  $P_e$  and the peak voltage  $u_{pk}$  at the transducer terminals and measuring the

generated *SPL* output while reproducing a multi-tone signal with a spectrum  $G_w(f)$  and crest factor  $CF_w$  as specified in the typical stimulus used in the previous design steps.

The cancelation of the nonlinear distortion can easily be checked by analyzing the spectral components at frequencies not excited in the sparse multi-tone stimulus. Standard techniques [21] can be applied to measure harmonic distortion, intermodulation and impulsive distortion indicating voice coil rubbing, air leakage noise and other loudspeaker defects.

Evaluating the distortion reduction in music or any other audio stimulus having a dense spectrum requires a system identification technique [25] that separates the nonlinear distortion (residuum) from the desired linear component. The residuum can be analyzed in the time and frequency domain and is the basis for perceptual modeling, distortion auralization [24] and a systematic listening test [26] to determine audibility and annoyance of the remaining distortion components.

The adaptive loudspeaker system based on current monitoring allows a stand-alone self-test on a variety of program material to check assumptions made in the design process, while assessing aging of the suspension and the long-term performance other critical hardware components.

## 7.6 System Optimization

The evaluation above provides valuable information for optimizing the target specification and selecting or designing better hardware components. If there is no time for significant changes, a modification of the protection parameter and the target alignment in the control software can be used to cope with unknown limitations in the hardware components. This usually requires an additional iteration of the last steps 7.4 and 7.5 in the design process. For example, voice coil rubbing occurring at higher amplitudes can be avoided by reducing the peak displacement  $x_{max}$  in the mechanical protection system. If the transducer has a lower power handling than expected due to blocked heat transfer in the cabinet, the thermal protection system can provide a fast-interim solution until a more efficient transducer with improved air convection cooling [7] is available.

In some applications such as high-quality audio, active noise and echo cancellation, the attenuation caused by the activated protection system is undesired. Here, keeping the overall response  $H_o(f)$  within the highly efficient frequency band reduces the need for mechanical and thermal protection.

## 8 Conclusion

The electro-acoustical efficiency is an important criterion for evaluating the transducer and system design with respect to the optimal use of all resources. Most of the electrical input power will be converted into heat and only a small fraction (far below 1% in micro-speakers) will be radiated as sound power. Increasing efficiency is the key to generating more output in smaller loudspeaker systems and reducing power consumption in portable applications with limited battery capacity.

Efficiency is not identical with voltage sensitivity. The frequency dependent efficiency  $\eta(f)$  and voltage sensitivity  $SPL_{1V,1m}(f)$  are required to estimate acoustical output power and the peak voltage capabilities of the amplifier for a broadband stimulus with defined voltage spectrum  $G_u(f)$  and probability density function  $pdf(u)$ .

The lumped parameters of the transducer model measured or predicted by FEA are a suitable basis for evaluating design choices and investigating the influence on sensitivity and efficiency. The actual resonance frequency  $f_s$  and the quality factors  $Q_{TS}$ ,  $Q_{MS}$  and  $Q_{ES}$  of the transducer play a minor role in Green Speaker Design because those transducer characteristics are highly time-variant due to production variances, aging and external influences (climate) and can easily be compensated by adaptive control.

Thus, digital signal processing available in active audio devices changes the paradigm in passive transducer design. The second part [1] continues this approach and investigates the optimal design of the transducer and illustrates the potential of this approach in a case study.

## 9 References

- [1] W. Klippel, "Green Speaker Design (Part 2: Optimal Use of System Resources)," presented 146th Convention of Audio Eng. Soc., Dublin, Ireland, 2019 March 20–23.
- [2] G. Ramos, J. Lopez, "Filter Design Method for Loudspeaker Equalization Based on IIR Parametric Filters," J. Audio Eng. Soc., vol. 54, no. 12 pp. 1162-1178 (2006).
- [3] R. Small, "Direct Radiator Loudspeaker System Analysis," J. Audio Eng. Soc. vol. 20, no. 5, pp. 307-327 (1972).
- [4] G. Vignon and S. Scarlett, "Specifying Xmax for Micro-speakers and Smart Amplifiers", presented at the 137<sup>th</sup> Convention of the Audio Eng. Soc. 2014, Oct. 9-12<sup>th</sup>, Los Angeles, USA, preprint 9114.
- [5] W. Klippel, "Mechanical Overload Protection of Loudspeaker Systems," J. Audio Eng. Soc. vol. 64, no. 10, pp. 771 – 783 (2016).

- [6] K. M. Pedersen, "Thermal Overload Protection of High-Frequency Loudspeakers," Rep. of final year dissertation, Salford University, UK (2002).
- [7] W. Klippel, "Nonlinear Modeling of the Heat Transfer in Loudspeakers," *J. Audio Eng. Soc.* vol. 52, no. 1/2, pp. 3-25, (2004).
- [8] W. Klippel, "Loudspeaker Nonlinearities – Causes Parameters, Symptoms," *J. Audio Eng. Soc.* vol. 54, no. 10, pp 907 – 939 (Oct. 2006).
- [9] W. Klippel, "The Mirror Filter - a New Basis for Reducing Nonlinear Distortion Reduction and Equalizing Response in Woofer Systems", *J. Audio Eng. Soc.* vol. 32, no. 9, pp. 675-691, (1992).
- [10] W. Klippel, „Active Compensation of Transducer Nonlinearities,” presented at the 23rd Int. Conference of the *Audio Eng. Soc.* on “Signal Processing in Audio Recording and Reproduction”, Copenhagen, Denmark, (2003).
- [11] W. Klippel, “Adaptive Nonlinear Control of Loudspeaker Systems,” *J. Audio Eng. Soc.* vol. 46, pp. 939 - 954 (1998).
- [12] W. Klippel, “Mechanical Fatigue and Load-Induced Aging of Loudspeaker Suspension,” presented at the 131<sup>st</sup> Convention of Audio Eng. Soc. 2011, Oct. 20-23, NY, USA, preprint 8474.
- [13] F. Agerkvist and B. R. Pedersen, “Time-varying Behavior of the Loudspeaker Suspension: Displacement Level Dependency,” presented at the 127<sup>th</sup> Convention of the Audio Engineering Society, New York, October 2009, preprint 7902.
- [14] W. Klippel, “Nonlinear Adaptive Controller for Loudspeakers with Current Sensor,” presented at the 106<sup>th</sup> Convention of the Audio Eng. Soc., Munich, May 1999, preprint 4864.
- [15] W. Klippel, “Adaptive Stabilization of Electro-dynamic Transducers,” *J. Audio Eng. Soc.* vol. 63, no. 3, pp. 154-160 (2015).
- [16] L. Beranek, T. Mellow, “Acoustics: Sound Field and Transducers,” Academic Press, Amsterdam, 2012.
- [17] D. B. Keele, “Maximum Efficiency of Direct Radiator Loudspeakers,” presented at the 91<sup>st</sup> Convention of the Audio Eng. Soc., Oct. 1991, preprint 3193.
- [18] U. Skov, R. Christensen, “An Investigation of Loudspeaker Simulation Efficiency and Accuracy Using a Conventional Model, a Near-to-Far-Field Transformation, and the Rayleigh Integral,” presented at the 136<sup>th</sup> Convention of the Audio Eng. Soc. (April 2014), preprint 9057.
- [19] D. A. Anderson, “Driver-array Based Flat-panel Loudspeakers: Theoretical Background and Design Guidelines,” PhD thesis, University of Rochester, (2017).
- [20] N. J. Harris, and M. O. J. Hawksford. "Introduction to Distributed Mode Loudspeakers (DML) with First-Order Behavioral Modelling." *IEE Proceedings-Circuits, Devices and Systems*, vol. 147, no. 3, pp. 153-157, (2000).
- [21] IEC 60268-21: Sound System Equipment – Part Acoustical (Output Based) Measurements, draft 2017
- [22] IEC 62458:2010 Sound System Equipment – Electro-acoustical Transducers – Measurement of Large Signal Parameters.
- [23] Large Signal Identification (LSI), module of Klippel Analyzer System, Klippel GmbH <https://www.klippel.de/products/rd-system/modules/lsi3-large-signal-identification.html>
- [24] W. Klippel, “Auralization of Signal Distortion in Audio Systems, Part 1: Generic Modeling,” presented at the 51<sup>st</sup> Int. Conference of the Audio Eng. Soc. on “Loudspeakers and Headphones” , Helsinki, Finland, (August 2013), paper no. 2-1.
- [25] S. Irrgang, W. Klippel, “Audio System Evaluation with Music Signals,” presented at International Conference on Automotive Audio 2017 of the Audio Eng. Society (August 2017), paper no. P4-2.
- [26] Audio Engineering Society, "AES20-1996: AES recommended practice for professional audio - subjective evaluation of loudspeakers ", *J. Audio Eng. Soc.* vol. 44, no. 5, pp. 382-400 (reaffirmed 2007).